White Paper:

Effect of Surge Voltage Risetime on the Insulation of Low Voltage Machines Fed by PWM Converters

Rockwell Automation
Reliance Electric

Effect of Surge Voltage Risetime on the Insulation of Low Voltage Machines Fed by PWM Converters

Abstract: **This paper investigates the repetitive surge voltage withstand of low voltage mush wound machines operated on Adjustable Speed Drives (ASD) using Insulated Gate Bipolar Transistor (IGBT) semiconductor technology. Historical work on surge testing of motor insulation has focused on one or more of the following aspects; large hp motors, medium voltage form wound motors, single shot impulse type transients or low voltage machines with surge risetimes > 200 ns. IGBT drives can have risetimes of 50 ns to 200 ns. Thus, a new study on electrical stress of insulation systems due to the nonlinear voltage distribution of mush wound motors when subjected to repetitive steep dV/dt square pulse waveforms (rather than impulse wave testing) is presented. Magnitude and risetime of the repetitive ASD surge voltage transient induced on the machine terminals is reviewed first. Next, surge propagation into the winding was investigated to identify maximum voltage stress points on the conductor insulation. Potential failure mechanisms observed at these points are then discussed. The significance of decreasing surge risetime and increasing cable lengths on internal non-linear voltage distribution is studied with experimental results from a 7.5 hp motor with a tapped stator winding.**

I. Introduction

A. Motivation for ASD - Motor Surge Voltage Study

There is a long and rich history of studies done regarding the effect of surge voltages on machine insulation. Researchers in the 1920's recognized the presence of abnormal surge voltages and proposed preventive measures [1]. A rigorous analysis of surge voltage propagation and distribution on internal voltage stress in windings was done in the 1940's [2]. There have been many studies done (too numerous to accurately acknowledge them all) on surge voltage distribution in windings. For the most part, they have been done on large hp form wound medium voltage motors with the IEEE 1.2 / 50 μs surge impulse voltage wave of Fig. 1 applied to the terminals [3-9].

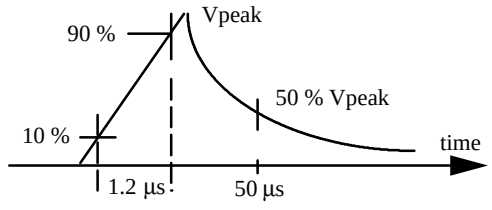

Fig. 1 "Lightning surge" impulse magnitude, risetime and duration

Investigation of non repetitive surge impulse type withstand on sinewave powered low voltage machines was done in the 1970's. This data was summarized in [11] and officially recorded by an IEEE working group in [12].

Investigation of repetitive surge voltage withstand on ASD powered low voltage mush wound machines was done in the 1980's with 480 V Current Source Inverter (CSI) drive technology [13]. This drive produced a 1,200 Volt spike with a 400 μs risetime at a rate of six times per 60 Hz cycle. This slow risetime allowed a linear distribution of voltage across the windings which, although increased the volts per turn stress, was far below destructive levels. Laboratory life tests and field experience has shown this to be the case. Pulse Width Modulated (PWM) ASDs using Bipolar Junction Transistors (BJT) with risetimes of 1 to 2 μs were popular in the late 1980's. These drives applied steep fronted voltages to the motor with dV/dt in the 500 V/μs to 1,200 V/μs range. The effect of this risetime on the nonlinear voltage distribution within mush wound motor windings was initially discussed in [14,15]. NEMA MG-1 Part 30 specifies 1,000 Vpk with a 2 μs risetime for general purpose motors. PWM BJT drives had few failures over the past ten years, although the voltage stress was greater than for CSI technology. Section IIB analysis shows that a 480V drive with 300 ft of output cable and BJTs of 1 μs risetime will have only a 30% overshoot transient above the dc bus level or 1,000 Vpk.

The reason for the work described in this paper is to investigate the repetitive surge voltage withstand of low voltage mush wound machines powered by the 1990's preferred drive of choice, a PWM ASD using IGBT technology with risetimes in the 50 ns to 200 ns range. Steep fronted voltage wavefronts applied to the 460V motor now have dV/dt's in the 6,500 V/μs to 13,000 V/μs range. NEMA MG-1 Part 31 specifies 1,600 Vpk with a 0.1 μs risetime for new inverter duty motor designs at this time [16]. This paper investigates the effect of sub-microsecond risetimes on the non-linear voltage distribution within the winding to determine the dielectric limitations of present motors and to determine insulation system requirements to meet inverter application needs.

B. Terminology

Before describing the specific motor which was tested, it is important to clearly define the terminology being used in reference to the induction motor windings. The terms used in this paper are as defined below.

Coil - A motor winding is made from a series of coils. Each coil is made from multiple turns wound around forms or pins to form a coil shape but with fairly random wire placement within the coil.
Turn - One complete loop of a conductor (wire). Each turn may consist of a single strand of conductor or multiple (parallel) strands. The conductor is normally insulated with enamel to separate each wire from the other.
Phase leg - In a 3 phase winding pattern, 3 different legs of coils are formed and connected. These may be series or parallel combinations of coil groups. The ends of the coils will be connected into a WYE or DELTA configuration with three leads as power input. For a WYE connection, the sinusoidal rms voltage across the leg equals line voltage divided by the square root of 3, but for a DELTA connection the leg voltage is equal to line voltage.

Group - Each phase leg is made up of an equal number of groups. The number of groups equals the number of poles times the number of phases. For 3 phase motors a 2 pole has 6 groups, a 4 pole has 12, and so on. In each group there are coils connected in series. The number of coils per group is determined by the number of poles, the number of slots in the stator and whether the winding pattern is single layer , two layer, or combination of single and two layer. For a standard two layer 4 pole winding with 48 stator slots, the number of coils in a group equal the number of slots divided by the number of groups or 4 coils per group in series.

Phase insulation - Each leg, or phase, of a three phase winding must be insulated from each other to keep the voltage potential between the wires low. Since the coils are inserted into the stator in such a manner as to have coils from different phases pass each other, and since the voltage across phases is always line value, all surges and high voltage conditions would stress the wire insulation. Insulation is used at each place in the winding where conductors would otherwise touch conductors from another phase.

Endturns - As the coils are placed in the stator slots, the ends of the coil extend beyond the core and span across to another slot for the placement for the other side of the coil. Both sides of each coil rest within a slot and the ends of the coils form the endturns or coilhead. The midstick within the slot separate the coil sides, while the phase insulation separates the coils in the endturn.

Concentric - Most machine windings are wound with coil patterns that are concentric. A concentric pattern is coils in a group wound with a large outer coil and the next coil fitting within the larger outer coil, etc. There is intended to be no crossover of coils within a group. This winding pattern may result in single coil sides in a slot which eases winding insertion.

Lap - This is the standard configuration for most hand windings. This pattern starts with all coils of equal size and shape. As each coil is inserted into the stator slot the first side of the coil goes into the bottom of the slot and the other side is placed in the top of another slot. Midstick insulation is placed between the bottom coil side and top side. Each coil overlaps the previous coils and results in a series of overlapping coils laying next and between other coils. As stated earlier, phase insulation is placed between coils of different phases in the endturns where they overlap each other.

Two layer & single layer - In the standard hand winding pattern the total number of coils is equal to the number of slots. Since a coil has two sides, each coil is in two slots. This means that coil sides must share slots and results in two coil sides in each slot. It is possible however to arrange a winding pattern with half the number of coils wound in a concentric pattern such that each coil side does not share a slot and fills the entire slot. This is known as a single layer pattern. There are also concentric patterns that result in some slots being shared while others are full to form a mixture of single and shared.

Hand inserted - Most hand windings are lap type winding patterns. After the coils are wound they are inserted by hand placing each side into a slot and hand placing the insulation for midsticks and phasing as the coils are inserted. The coils are layered and formed as they are inserted.

Machine inserted - If the coils are designed into a concentric pattern it is possible to wind the coils and insert using a machine for the entire process. If the winding is single layer the placement of midsticks is not required and the insertion is simplified although it is possible to wind and machine-insert midsticks. Virtually all machine wound windings are concentric coil patterns.

Mush Winding - Windings which employ round wires of a relatively small cross section are often referred to as mush or random windings. It is impractical to layer round wires in such a manner as to have even stacks of conductors layered on each other. In the endturns, wires will tend to cross over wires of adjacent coils.

Form Winding - Coils wound with wire that has a square or rectangular cross section are wound in layers of stacked wires that can be held in the original shape even when placed in slots. The coils are formed and placed in the stator resulting in endturns that are very rigid. This construction results in each turn being progressively layered onto the other such that turns only contact the next turn and do not cross over to other coils.

C. Machine Construction

A 460 V, 7.5 hp, 6 pole motor, delta connected, mush wound, with 19 turns per coil, 18 coils per phase in series, and 8 taps in the line-end coil (as shown in Fig 2) was tested.

The arrangement of individual turns within a "round wire" stator is a function of the particular winding pattern. While most hand-inserted patterns are two layer lap windings, there are numerous possible machine-inserted winding patterns. One specific motor tested in this investigation utilized a pattern which contains alternating "half-slot" and "full slot" or "single" and "double" coils (Figure 2). This implies that while the winding contains a nominal 19 turns per coil, there are slots which in fact contain 38 (2 x 19) turns in a coil which fills the full slot. This coil of 38 turns is therefore a collection of wires which are in close proximity both in the slot as well as in the coil head (end turn) region.

For the data shown below, the turns numbered 1 through 19 are in slots 2 and 8, while turns 20 through 57 are in slots 1 and 9.

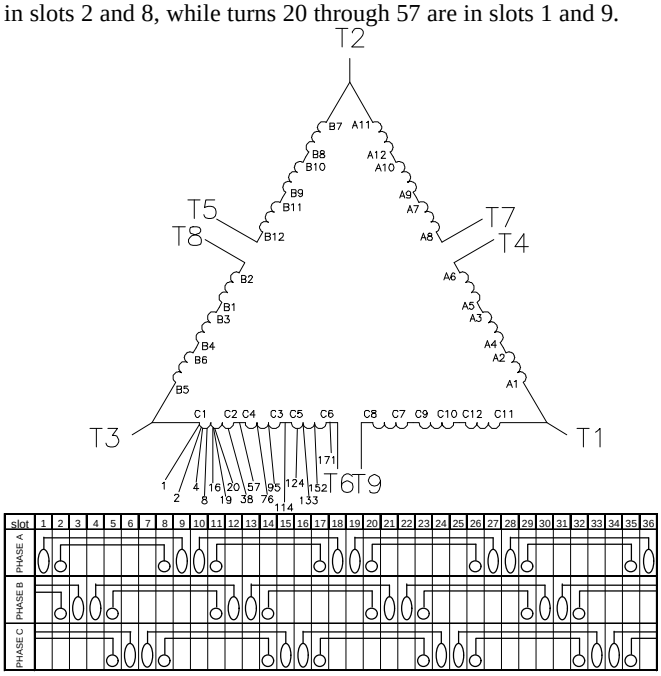

Fig. 2 Stator Winding layout /schematic of a mush wound 460V, 7.5 hp, 6 pole, test motor having tapped windings

D. Test Setup

Waveforms of the internal motor voltage distribution from T3 to the internal taps were recorded for a drive connected to a motor with a 5 foot motor cable. Drive risetimes were selected as 50 ns, 200 ns, 400 ns, 800 ns and 1.8 μs. The process was repeated for 100 foot and 300 foot cables. A 15 Volt controllable wave source was also used to supply fast rising voltage wavefronts to the motor terminals. First, magnitude and risetime of the ASD induced transient on the external motor terminals is reviewed. Experimental results of a tapped stator winding motor subjected to various IGBT drive risetimes provides an indication of where maximum voltage insulation stress internal to the motor occurs. Knowing the

maximum voltage stress point and the corona inception point of the insulation system allows one to determine a repetitive maximum dielectric withstand vs. risetime envelope for that particular motor.

II. Electrical Stress on Motor Insulation

A. Risetime Definition Of ASD Surge Voltage Transient

Motor overvoltage risetime is defined by NEMA MG-1 Parts 30, 31, depicted in Fig. 3. Drive output pulse risetime (t_{rise}) to the V_{dc} steady state dc bus level is determined by semiconductor switching times. This pulse is assumed to be applied to a distortionless transmission line cable (valid to 1,000 ft), so that motor terminal voltage risetime to the steady state voltage is identical to drive t_{rise}. Transient oscillation frequency (fo) at the motor terminals is superimposed upon the V_{dc} level and is actually set by cable length and cable construction [18-20]. Typical fo values range from 1 MHz @ 100 ft. to 100 kHz @ 1,000 ft for bundled PVC wires. The second slope from the steady state dc level to the transient peak will therefore change depending on cable length. Thus, a 10% to 90% of V_{dc} definition is presently used for t_{rise} to avoid confusion over variable test conditions, as well as to maintain consistency with the IEEE definition of risetime. Test results of section III A and III B show that faster drive output risetimes result in higher voltage stress on conductor insulation of the first to second coil group and first coils of the line end group. The effect of higher voltage stress on insulation failure is examined in Section II D and IV B.

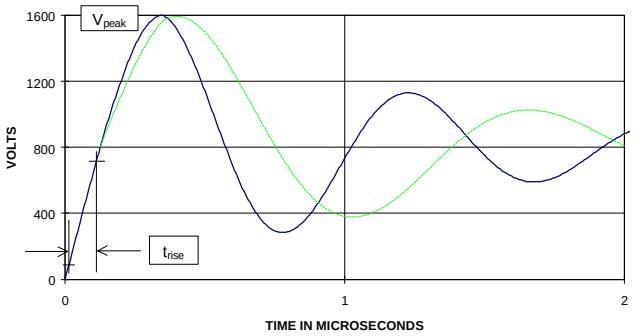

Fig. 3 NEMA MG1-Part 31 Peak Voltage and Risetime, plus Slope Change

B. Magnitude Of ASD Surge Voltage Transient

The transient peak voltage of Fig. 3 is due to reflected wave voltage at the motor terminals. Factors affecting peak terminal overvoltage are discussed in [21-23] and are as follows.

- Motor & Cable surge impedance
- Cable Length
- Cable Damping
- Risetime of Drive Pulse
- Magnitude of Drive Pulse
- Spacing of PWM Pulses

Fig. 4 shows drive pulse risetime determines a critical cable distance (l_C) where theoretical 2 pu overvoltage is developed for an initially uncharged cable condition [18,20]. A BJT drive with t_{rise} = 2 µs develops 2 pu motor voltage transients at a l_C of 1,200 ft whereas an IGBT drive with t_{rise} = 0.1 µs generates 2 pu at l_C = 80 ft. Cable lengths < l_C develop less pu overvoltage than 2.0 .Fig. 4 and Fig. 5 show that motor terminal voltage increases in a quarter sinewave fashion from 1.0 pu at zero cable length to the peak value of 2.0 at l_C .

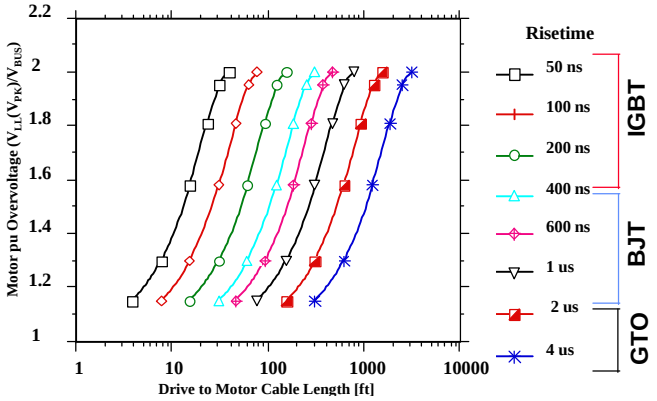

Fig. 4 Motor pu Overvoltage vs. Cable Length and Risetime

Cable lengths >l_C in Fig. 5 develop at least the pu magnitude of 2.0, and possibly greater values, depending on the spacing of PWM pulses [19,22]. Motor terminal voltage > 2 pu may occur for cable lengths > l_C , depending on the zero voltage spacing of the line to line PWM pulses. This is a result of trapped charge from the previous transient not fully decaying to zero before the next pulse arrives. High carrier frequencies (f_C) do not affect the < 2 pu peak transient for cable lengths < l_C. However, a high f_C spaces the pulses closer together, thus generating measured transients to 3 pu in the > l_C range of Fig. 5. Cable ac resistance damping of different AWG wires influence residual trapped charge on the cable and thus only affect peak transient magnitude in the > l_C. range. Other interactions between PWM modulators and cable parameters that create > 2 pu transients, such as polarity reversals, are detailed in [18-20].

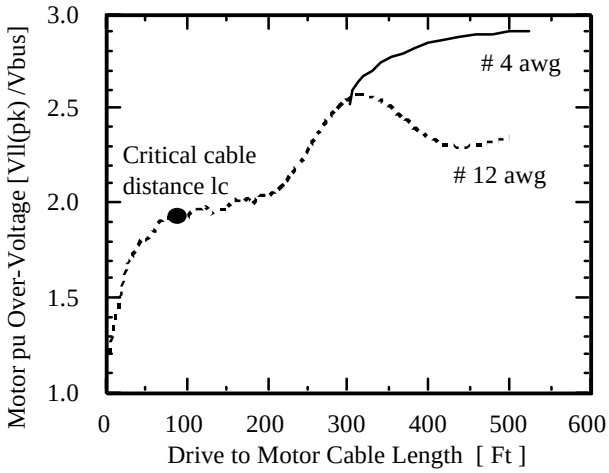

Fig. 5 Typical motor pu overvoltage vs. cable length

Table I shows that the magnitude of the drive V_{dc} pulse directly influences peak transient voltages at the motor terminals. Table I also shows that the NEMA MG-1 Part 31 specification does not cover all 2 pu and 3 pu contingencies, especially for 575 V systems and high line conditions.

Thus, motor line-to-line transient voltages of 2 pu magnitude are possible on every pulse edge, at a rate determined by the IGBT f_C

selected (f_C ~ 2 to 15 kHz). Critical cable distances l_C where 2 pu occurs, range from 50 ft for IGBT t_{rise} = 50 ns to 150 ft for t_{rise} = 200 ns. Terminal transients of 3 pu are possible at distances beyond l_C and for high values of f_C selected. How this peak external terminal voltage divides across turns and coils internal to the motor is determined by the surge propagation velocity into the winding.

Table I. Comparison of Possible Transients vs. NEMA

AC System Voltage	Vdc bus	2 pu Vpk	3 pu Vpk	NEMA MG1-Part 31
480V+10%	715	1,430	2,150	1,600V_{pk} @0.1μs
575V+10%	860	1,720	2,580	1,600V_{pk} @0.1μs

C. Surge Propagation Velocity in a Mush Wound Machine

Drive to motor cables may be modeled by homogeneous L - C ladder networks. Machines do not have homogeneous and symmetric L - C structures because they contain elements such as single turns, coils, groups and layers that are interconnected to form a winding. An inverter pulse penetrates from the exterior terminals into this winding via two modes, traveling wave and oscillatory. The in-homogeneous structure of the winding elements cause a considerable change in pulse shape internal to the winding.

Winding propagation velocity υ of the traveling wave mode is simply expressed as $\upsilon = 1 / (L\ C)^{0.5}$ and characterized by partial inductance L and capacitance C of each element. The majority of conductor capacitance is in the stator core slots to ground with minimal capacitance to ground from the endturn wires outside the stator core. The majority of conductor inductance is due to the self and mutual inductance of the conductors in the end turn portion outside the stator core. Slot self inductance is minimal because of magnetic skin effect in the steel core. Rapidly changing stray flux lines due to the traveling pulse risetime, do not fully penetrate the core and are thus confined to air spaces around the slot conductors.

The initial turns of a winding can be driven into an oscillatory mode if the equivalent frequency of the pulse risetime [$f_{rise} = 1 / (\pi t_{rise})$] excites the natural frequency of the winding. This mode is discussed later in Section III A.

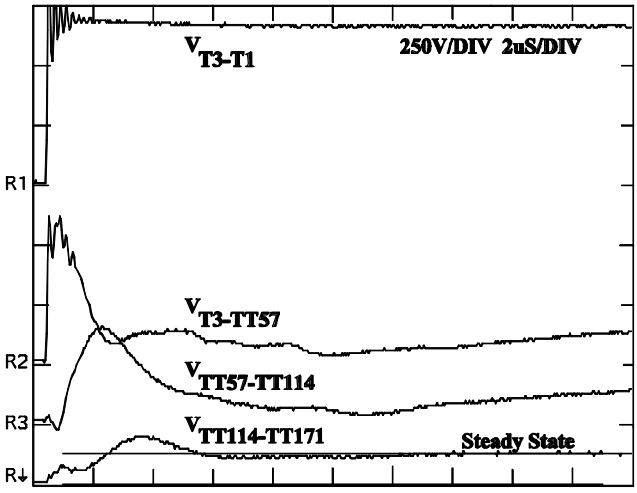

Fig. 6 Voltage distribution across first 3 coil groups vs. time for a 670 Vpk pulse with a risetime of 50 ns

Fig. 6 demonstrates magnitude and slope changes across the first three coil groups of the Fig. 2 mush wound machine for an incoming 670 Vpk inverter pulse with a 50 ns risetime and 5 ft. motor cable. Voltage risetime across the first coil is 50 ns, while coils 2 and 3 have slower risetimes of 1.28 μs and 2.25 μs. Peak voltage across the first coil group is 90% of incoming pulse voltage and contains some oscillatory modes, while coil groups 2 and 3 are predominantly traveling wave modes with peak voltages of 60% and 25% of applied pulse magnitude.

Propagation time (t_p) from coil group 1 to 2 in Fig. 6 is 480 ns while t_p from coil group 2 to 3 is 2.4 μs. Propagation velocity $\upsilon = \Delta x / \Delta t_p$ and equates to 72 m/μs (24% υ_o) from coil group 1 to 2 and 18 m/μs (6% υ_o) from coil group 2 to 3. These values agree with mush wound machine analysis stating typical values of 5% - 15% of υ_o. Bundled cables have a υ = 50% υ_o, while υ_o = 300 m/μs is the wave propagation velocity of separated transmission lines in air.

The key point is that highest internal transient voltage stress occurs from coil group 1 to coil group 2. Transient risetime determines what percentage of the external line to line transient voltage appears across the first coil and if a resonant oscillation frequency of the first turns of the line end winding is excited. Full peak transient voltage at the terminals may be applied across the line end coil for t_{rise} = 50 ns.

D. Motor Failure Mechanisms Due to ASD Voltage Transients

Primary components in the insulation systems of mush wound motors include stator magnet wire insulation, stator resin system, phase / group insulation, and slot insulation. Potential failure modes of the insulation system are phase to ground, phase to phase, turn to turn, or coil to coil. Insulation system failure occurs when the magnitude and risetime of the repetitive transient voltage stress exceeds the insulation system's withstand capability. The dielectric failure mechanism limiting long term withstand capability to repetitive transients is not typically the single shot ultimate "breakdown voltage strength" of insulation, but a lower limit imposed by partial discharge or corona [17,22,25-30].

Corona Inception Voltage (CIV) is the minimum applied voltage at which partial discharges occur, that is, the lowest applied voltage that causes ionization of the air around conductors. On reaching a critical voltage gradient of the air, a partial discharge occurs. Ion bombardment and resulting ozone attack erodes the organic surfaces until the dielectric withstand is below the magnitude of the peak voltage stress and catastrophic failure occurs. The term corona is sometimes used at higher energy levels when visible light around conductors is emitted. Time to failure is fairly rapid when applied voltages exceed the insulation system CIV level at the operating temperature.

AC induction motors without proper phase insulation operated on inverter supplies have a high incidence of failures. These failures are phase-to-phase, although the location of the failure point within each phase will determine if it looks like a "dead short," or just an "unbalanced resistance."

In the case of motors which are properly insulated phase-to-phase, the fast risetimes and high peak voltages can create a failure mode based on partial discharge erosion of the magnet wire insulation. This failure mode is based on high voltage gradients as discussed above. The breakdown of insulation will most commonly occur in the endturn region, where wires from different coils can come into contact (Fig 7).

A line to ground insulation failure mode as the initiating cause of motor failure is rare. Peak $V_{l\text{-}g}$ stress from IGBT ASDs is typically at or below the line to ground CIV levels of most motors [25].

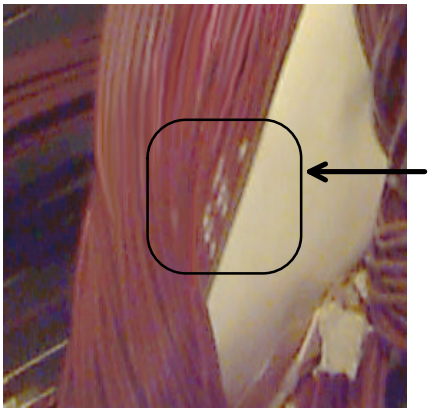

Fig 7 Effects of corona

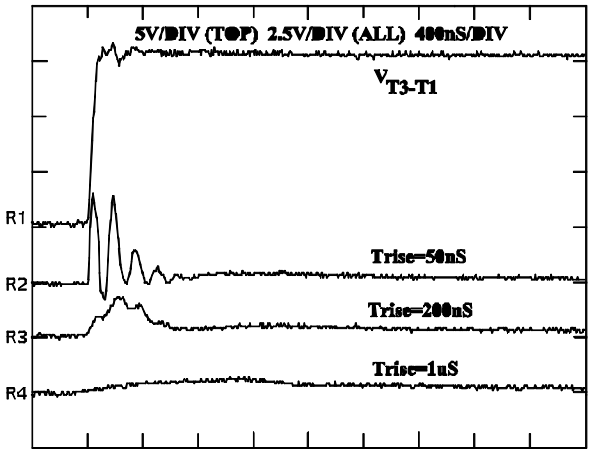

Fig. 8a Oscillatory propagation of voltage across first 4 turns vs. time for a 15 Vpk pulse with various risetimes

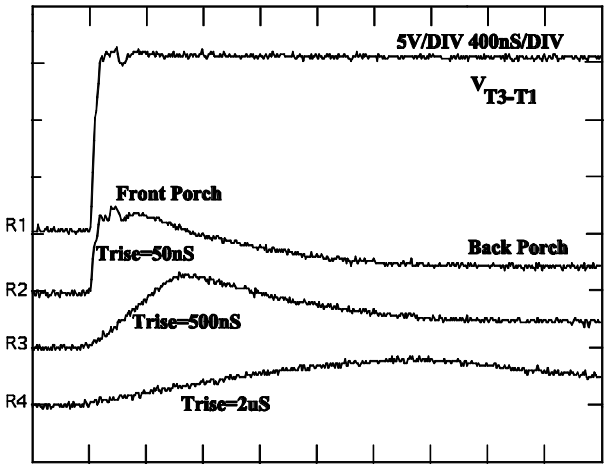

Fig. 8b Traveling wave propagation of voltage across first coil group vs. time for a 15 Vpk pulse with various risetimes

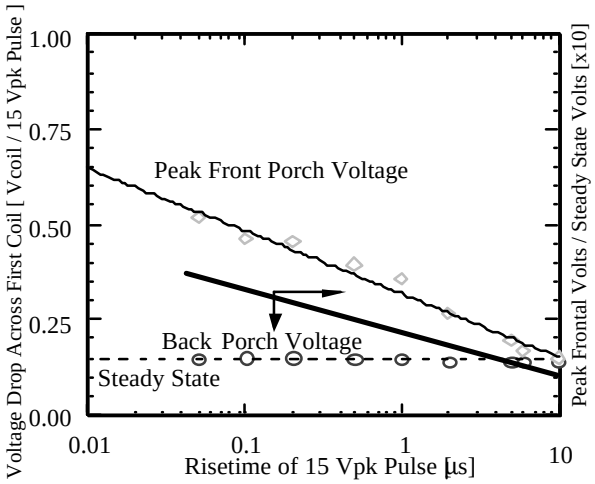

Fig. 9 Voltage drop across first coil group vs. 15 V pulse risetime

III. Effect of Risetime on Voltage Distribution

Test results on the non-linear voltage distribution of the tapped stator winding motor are examined in this section. Initial testing was done with single shot, low voltage, pulses of various risetimes to identify trends. Next, winding voltage distribution was recorded for a 480V PWM inverter of various output risetimes that was connected to the test motor with both short and long cables for a no load current condition.

A. Experimental Results - Low Voltage Pulse Testing

Low voltage (~1 Vpk) pulse testing has been used to determine voltage distribution data on a 6 kV motor [9]. In our investigation, a 15 Vpk to zero, 1 kHz square pulse generator was applied to motor terminals T3(+) - T1(-) of Fig. 2, with coil leads T5-T8 and T4-T7 connected. Fig. 8a shows the voltage across the first few turns that are in close proximity, from T3 to Tap Turn 4 (TT4), for various risetimes. Risetimes < 0.4 μs, and especially < 0.1 μs in Fig. 8a, excite a 20 - 30 MHz oscillatory mode of propagation into the line end winding. Thus, pulse risetime may cause a resonant condition where transient voltage stress greatly increases over the steady state stress of (TT4 / 342 Total Turns) x applied dc peak.

Fig. 8b shows voltage across the first coil group (57 T) for various risetimes, while Fig. 9 plots data from these waveforms. The traveling wave mode of propagation is evident, while the oscillatory mode has disappeared. Peak frontal overshoot voltage increases as risetime decreases. The back porch of the traveling wave was always the steady state value of 57T / 342T x 15 Vpk or 0.166 pu for any risetime, as in Fig. 9. The slow moving oscillation around the backporch in Fig. 8b is really due to a traveling wave set up from T3 to T2 and returning toward T1. This traveling wave adds or subtracts within the T3-T1 winding with the original T3-T1 traveling wave initiated to give the impression of a slow oscillation. Disconnecting coil leads T5-T8 and T7 -T4 eliminated this phenomenon. Peak overshoot voltage is 1/2 of applied T3-T1 peak for t_{rise} = 0.05 μs, but approaches the steady state value for t_{rise} = 5 μs in Fig. 9, while a t_{rise} = 10 μs eliminates any overshoot. Thus, from low level testing a t_{rise} = 0.05 μs pulse has transient voltage stress 4x greater than steady state from Fig. 9.

Fig. 10a plots low level test data from T3 to various tap turns up to the end of the first coil lead (57 Turns, winding pu = 0.166). The first few (4) turns (TT4 winding pu = 0.0117) actually have relatively low stress if t_{rise} > 0.5 μs, due to elimination of winding resonance. Voltage stress at TT4 is 3x greater for t_{rise} = 0.05 μs than for t_{rise} = 0.2 μs and 26x greater than the steady state stress (0.3 pu / 0.0117 pu). Risetimes of 5 μs and 10 μs lie almost on top of the theoretical linear division line at every tap. Thus, based on low level testing, the maximum voltage stress across the first coil group ranges from steady state stress of 0.166 pu to 0.5 pu of applied peak magnitude for square pulses with risetimes from 10 μs to 50 ns, respectively.

Fig. 10b plots low level test data from T3 to various tap turns up

to the end of the third coil group. The significance of this chart is that all the risetimes converge toward the steady state values at the end of the 3 rd coil group (1/2 the total winding) due to oscillations dying out and traveling wave reflection amplitudes decreasing as the wave penetrates into the winding with slower risetimes.

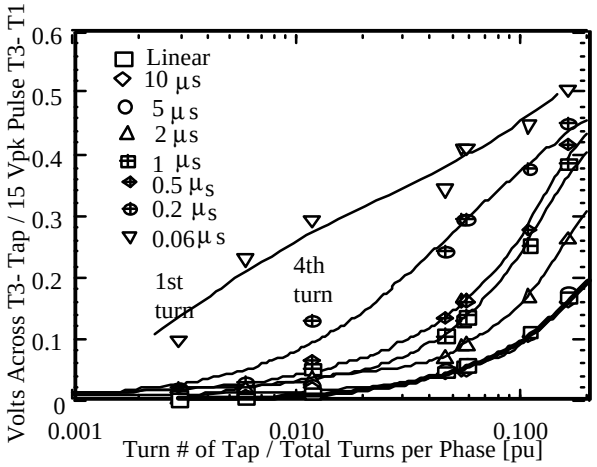

Fig. 10a PU voltage drop across taps of first coil group vs. pu tap location for various 15 Vpk pulse risetimes

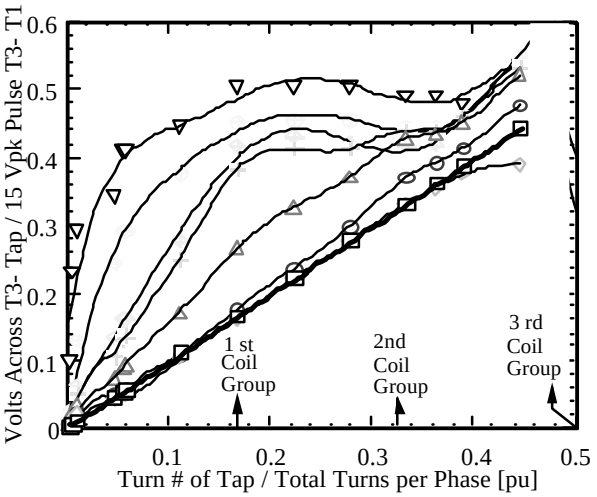

Fig. 10b PU voltage drop across taps of entire winding vs. pu tap location for various 15 Vpk pulse risetimes

B. Experimental Results - Inverter Testing with Short Cables

A 3 phase, 480V (660 Vdc bus), 2 kHz, PWM inverter of various output risetimes was connected through a 5 ft cable to the tapped winding test motor at no load current conditions. The 5 ft cable length limits peak reflected wave voltage so only Vdc exists on the motor terminals for all t_{rise} tested. Maximum voltage distribution across the first 4 turns and across the first coil group were measured for all t_{rise} tested. Fig. 11 shows traces of voltage across the first turn and the first coil for t_{rise} = 0.05 µs. The pu voltage stress across the winding to a step pulse was essentially doubled as compared to low level test results. The difference may be due to the energy storage initial condition of having no load current flowing in the windings prior to the step.

Fig. 12a shows drive induced voltage stress across the first few turns are much greater as compared to the single phase low levels tests of Fig. 10a. Fig. 12a also shows the trend toward oscillatory peak resonant voltages as t_{rise} < 0.2 µs. However, the voltage

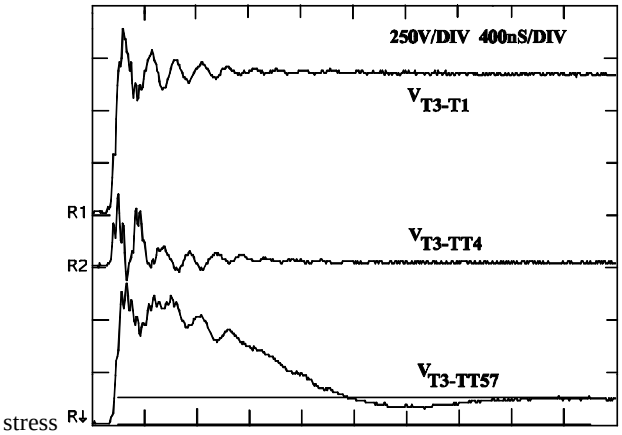

Fig. 11 Voltage across 1st turn and 1st coil group for 660 Vpk, t_{rise} = 0.05 µs pulses from PWM inverter with 5' cable

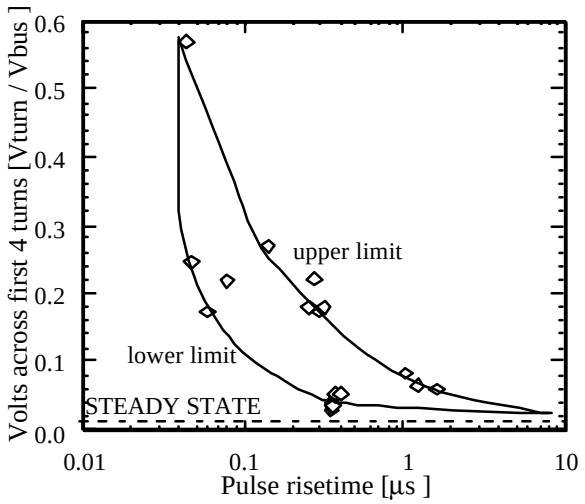

Fig. 12a PU voltage drop across first 4 turns vs. pulse risetime of 660 Vdc peak pulses from PWM inverter with 5' cable

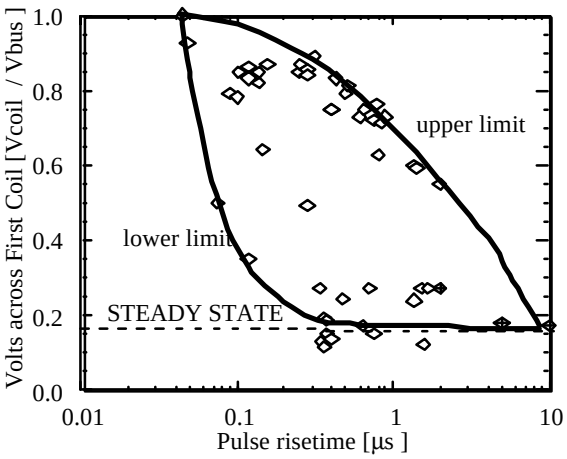

Fig. 12b PU voltage drop across first coil group vs. pulse risetime of 660 Vdc peak pulses from PWM inverter with 5' cable

for an IGBT t_{rise} = 0.05 µs now approaches a significant 0.6 pu of applied terminal voltage. This represents a 50X increase over steady state voltage stress {e.g., 0.6 pu / (4T / 342T)}. It may be inferred from Fig. 12a, as well as field results over the past ten years, that drives with risetimes of 1 µs to 2 µs never excited the first turn failure mode phenomenon.

Fig. 12b shows that drive induced voltage stress across the first coil group is also greater compared to the single phase low level tests of Fig. 10b. Fig. 12b also shows the trend toward higher voltage stress as t_{rise} is reduced from 5 μs to 0.05 μs. However, the voltage stress for an IGBT t_{rise} = 0.05 μs now approaches a significant full 1.0 pu of applied terminal voltage. This represents a 6X increase over first coil group steady state voltage stress {e.g., 1.0 pu / (57T / 342T)}. There was an upper and lower voltage stress band for each output pulse risetime measured. The upper limit measurement occurred when line phase current was entering terminal T3. Likewise, the lower limit correlated when phase current was leaving terminal T3. It is speculated that the lower limit is the result of a positive step pulse initiating a forward traveling voltage wave into the winding, interacting with the reverse counter-emf kick voltage across the winding trying to maintain current in the same direction prior to the new step.

It may be inferred from Fig. 12b that previous generation drives, with risetimes of 1 μs to 2 μs, had first coil group voltage stress between steady state levels (lower limit) and 0.55 pu of applied terminal voltage (upper limit). Likewise, present IGBT drives, with risetimes as low as 0.05 μs have first coil group voltage stress between 0.55 pu (lower limit) to 1.0 pu (upper limit) of applied terminal voltage.

The faster switching speeds of IGBT drives has reduced drive watts loss, reduced package size and increased carrier frequency for better ripple current performance. As compared to BJT drives, the effect of this faster converter risetime has been to nearly double voltage stress in a primary failure area, e.g.. wires in the first few coil groups.

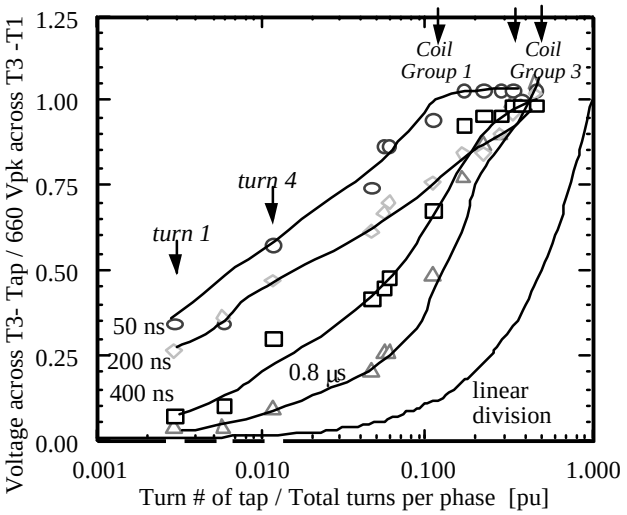

Fig. 13 PU voltage drop across taps of entire winding vs. pu tap location for 660 Vpk pulse risetimes, 5' cable

Fig. 13 plots the voltages from T3 to all taps in the winding. The significance of this chart is that all the voltages for the various risetimes do not converge toward the steady state linear division values at the end of the third coil group (1/2 the total winding) as in the low level testing, but rather converge toward a 2x higher value being applied peak terminal voltage value.

C. Experimental Results - Inverter Testing with Long Cables

Test conditions of Section III B were repeated with the exception that cable lengths were increased to 100 and 300 feet. These lengths now caused reflected wave peak voltages of 1,170 Vpk (1.77 pu) and 1,250 Vpk (1.89 pu) at the motor terminals rather than the 1 pu V_{dc} bus as before. The results of Fig. 14 show that for a given fixed risetime, the addition of long cables lower voltage stress on the initial turns but increases the stress further into the winding [31]. First coil group stress for t_{rise} = 200 ns, increased from 0.8 to 1.1 pu with the longer cables.

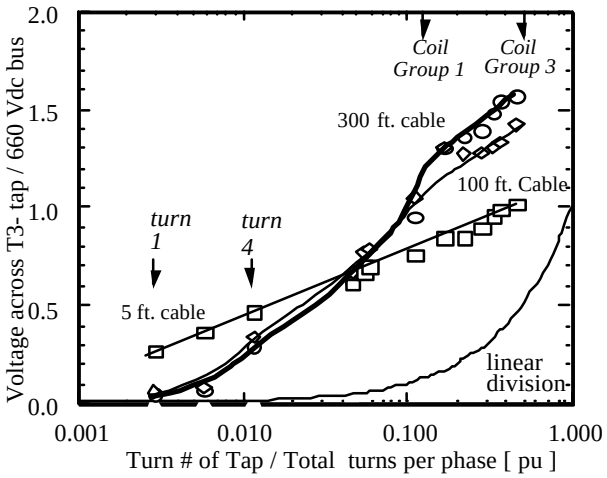

Fig. 14 PU voltage drop across winding for trise of 200 ns 660 Vpk pulse with 5, 100, and 300 foot cables

IV. Dielectric Withstand vs. Risetime Envelope

The 1981 IEEE dielectric withstand vs. risetime envelope was based on a survey of 60 Hz sinewave operated motors with standard insulation subjected to infrequent impulse transients. It is a guideline to determine acceptable motor life, when subjected to < 100 surges per year.

For ASD applications, the wires which may be subjected to the highest dielectric stress have been identified as the first and last turn of the first coil and the turns of adjacent coils within the line end coil group. The maximum voltage distribution across these high stress elements under PWM operation have been investigated for various pulse risetimes and cable lengths. Assuming partial discharge is a predominant failure mechanism, a peak voltage withstand vs. risetime curve may be generated for a given motor with a particular insulation system (Fig 15). This curve is a function of the insulation system CIV level.

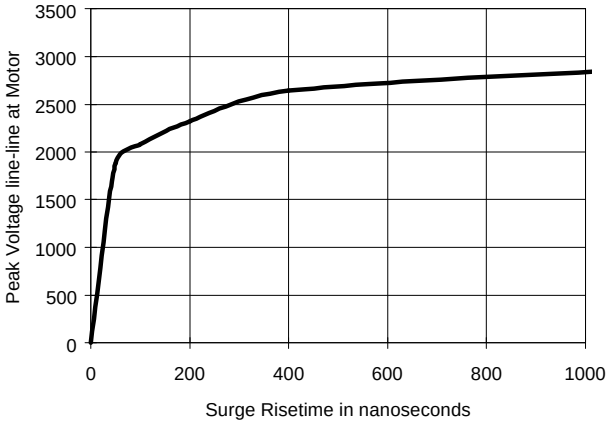

Fig. 15 Motor Peak Withstand Voltage based on NO Partial Discharges occurring

V. Conclusions

This paper reviewed the effects of repetitive transient voltage magnitude and risetime on low voltage mush wound motor insulation as a result of operation with high dV/dt square pulse wavefronts of PWM drives with risetimes from 50 ns to 10 μs.

The ASD-induced transient voltage pulse at the motor terminals was found to penetrate into the winding via oscillatory and traveling wave modes. Tapped stator winding results showed an oscillatory mode was evident only in the first few turns, and only for pulse risetimes < 0.3 μs. Pulse propagation into the winding via the traveling wave mode showed a non-linear voltage distribution. For t_{rise} = 50 ns, 80% of the terminal voltage appears across the first coil group (in a machine with 6 coil groups per phase). Differential pu coil voltages for t_{rise} = 0.05, 0.2 , 0.5 and 1 μs PWM pulses followed trends of a medium voltage motor subjected to impulse tests. Pulse propagation through line end coil groups have a wavefront initially equal to the applied t_{rise} and velocity approximately 25% the speed of light. Pulse propagation through remaining coils have significantly reduced risetimes, reduced peaks and traveled at only 5% υ_o. The highest voltage stress across any two conductors which may be in contact was found to exist from the first turns of the line end coil to the last turns of the coil group.

For motors manufactured with proper placement of phase insulation, the most probable failure is at the highest voltage stress points, i.e. the first turns of the line end coil to the last turns of the coil group. Partial discharge / corona is the predominant failure mechanism reducing life. Normal insulation life is possible if the repetitive voltage stress at these points is less than the CIV level of the motor insulation system.

The effect of risetime on winding voltage distribution using low level pulse tests revealed a 20 - 30 MHz oscillation across the first few turns that was excited by pulse risetimes < 0. 3 μs, and which increased peak voltage to 4 times greater than steady state stress. This oscillation did not exist after further wave penetration into the winding. Pulse test risetimes of 5 and 10 μs yielded winding transient voltage distributions approaching the steady state value. First coil group voltage stress for low level pulse risetimes of 0.05 μs yielded maximum transient voltages equal to approximately 0.5 pu of applied line to line pulse magnitude.

Voltage distribution vs risetime data, winding pattern data, and insulation system CIV data at operating temperature were used to generate an allowable peak surge voltage vs risetime curve based on corona limitations.

Acknowledgment

The authors wish to thank H. Jelinek and J. Pankau for their assistance in taking the multitude of measurements required to perform this study and in processing the data.

References

[1] Weed. J., Prevention of transient voltages in windings, AIEE Journal, Vol. 41, 1922, p. 14

[2] Rudenberg,R., Performance of traveling waves in coils and windings, AIEE Magazine , 1940, Vol. 59 , p 1031

[3] Sexton, R., A survey of turn insulation on large ac motors, IEEE 32C79-23

[4] McLaren, P., Abdel-Rahman, M., Modeling of large AC motor coils for steep fronted surges studies, IEEE Trans. Industry applications, Vol. 24, No 3, May 1988

[5] Al-Furaih, A. , Evaluation and testing of turn insulation of large AC motors, IEEE IAS Appl., Vol. 31, Jan. , 1995

[6] Gupta,B., Lloyd,B., Stone,G., Campbell,S., Sharma,D., Nilsson,N., Turn insulation capability of large AC motors - Part 1 surge monitoring, IEEE Trans. Energy Conversion Vol. EC-2, N0.4 , Dec 1987

[7] Gupta,B., Lloyd,B., Stone,G., Sharma,D., Fitzgerald,J., Turn insulation capability of large AC motors - Part 2 impulse strength, IEEE Trans. Energy Conv. Vol. EC-2, N0.4 , Dec 1987

[8] Gupta,B., Lloyd,B., Stone,G., Sharma,D., Fitzgerald,J., Nilsson, J., Turn insulation capability of large AC motors - Part 3 insulation coordination, IEEE Trans. Energy Conv. Vol. EC-2, N0.4 , Dec 1987

[9] Gupta,B., Sharma,D., Bacvarov,D., Measured propagation of surges in the winding of a large AC motor, IEEE Trans. Energy Conv. Vol. EC-1, N0.1 , March ,1986

[10] Christiansen, K. , Pedersen, A. , An experimental study of impulse voltage phenomena in a large AC motor, IEEE 68C6-EI-87 ,1968

[11] Nailen, R., Transient surges and motor protection, 0093-9994/79/1100-0606 , IEEE 1979

[12] IEEE Working Group Report , Impulse strength of rotating machinery", IEEE trans. PAS , 100, Aug. 1981

[13] Quirt, R. , Voltages to ground in load commutated inverters, IEEE Trans. Industry Applications, Vol. 24, No 3, May 1988

[14] Bonnet,A., Analysis of the impact of pulse width modulated inverter voltage waveforms on AC induction motors, 0-7803-2028-X-6/94 1994 IEEE

[15] Bonnet,A., A Comparison between insulation systems available for PWM inverter fed motors, IEEE Petroleum & Chemical Industry Conf.", Sept./96

[16] NEMA MG-1 Part 31, Rev 3, Specification for Definite Purpose Inverter fed Motors

[17] Kaufhold, Borner, Eberhardt, Speck, Failure mechanism of the inter turn insulation of low voltage electric machines fed by pulse controlled inverters, IEEE Electrical insulation magazine , Sept./ Oct. 1996

[18] Kerkman, R., Leggate, D., Skibinski,G., Interaction of drive modulation & cable parameters on AC motor transients, 1996 IEEE IAS Conf., Oct. ,1996

[19] Kerkman, R., Leggate, D., Skibinski,G., PWM modulators and their influence on AC motor transients, 1997 IEEE APEC Conf.

[20] Skibinski,G., Kerkman, R., Leggate, D., Cable parameters and their influence on AC motor transients, 1997 IEEE APEC Conf.

[21] Nelson,R., Skibinski, G., Solutions to sudden motor failures, Power Transmission Design, Aug./95

[22] Skibinski,G., Evon, S., Kempke,D., Saunders,L., IGBT drive technology demands new motor and cable considerations, IEEE PCIC Conf., Sept. 96

[23] Persson, E. , Transient effects in application of PWM inverters to induction motors, CH297-6/91

[24] Skibinski, G., Design methodology of a cable terminator to reduce reflected voltage on ac motors, IEEE IAS Conf., 1996

[25] Bell, S. , Sung,J., Will your motor insulation survive a new adjustable frequency drive, IEEE 1996 PCIC Conf., also IEEE International Electric Machine & Drives conf., May 1997

[26] Skibinski ,G. , Erdman, J., Pankau, J., Campbell, J., Assessing ac motor dielectric withstand capability to reflected voltage stress using corona testing, IEEE IAS Conf. , Oct 1996

[27] Oliver,J., Stone,G., Implications for the application of adjustable speed drive electronics to motor stator winding insulation, IEEE Electrical Insulation, Aug. 1995

[28] Rehder, R. Preliminary evaluation of motor insulation for variable speed applications,

[29] Hyypio, D., Simulation of cable and winding response to steep fronted voltage waves, IEEE IAS Conf., Oct. 1995

[30] Hyypio, D., A model for predicting voltage endurance of magnet wire film subjected to PWM voltage waveforms with transient overshoots, 1997 APEC conf, Feb, Atlanta.

[31] Gubbala,von Jouanne,A., Enjeti,P., Singh, Toliyat, H., Voltage distribution in the windings of an ac motor subjected to high dV/dt PWM voltage, IEEE PESC Conf April 1995

This document located at:
http://www.reliance.com/pdf_elements/b7103.pdf

Reliance Electric / 24800 Tungsten Road / Cleveland, Ohio 44117 / 216.266.7000 / http://www.reliance.com

Rockwell Automation
Reliance Electric

Printed in U.S.A. B-7103 1197